International Journal of Modern Manufacturing Technologies
ISSN 2067–3604, Vol. XIV, No. 2 / 2022
https://doi.org/ 10.54684/ijmmt.2022.14.2.40

CONTROL OF SHIP FIN STABILIZERS BY A PID CONTROLLER: A NUMERICAL ANALYSIS

Dumitru Deleanu, Constantin Louis Dumitrache, Mihaela Turof

Constanta Maritime University, Department of General Engineering Sciences, Mircea cel Batran street, No. 104, 900663, Romania.

Corresponding author: Dumitru Deleanu, dumitrudeleanu@yahoo.com

Abstract: The reduction of ship roll motion is important in order to prevent damage to cargo, to allow the crew to work efficiently and to provide comfort for the passengers. There are passive devices like bilge keels or anti – roll tanks and active devices like gyrostabilizer and stabilizing fins which are commonly used to generate an opposed moment to the wave and wind excitation roll moments in response to the command of a control system. The paper presents numerical results of using a Proportional - Integral – Derivative (PID) controller for damping the roll motion of a fishing boat equipped with a fin stabilizer system and sailing in regular waves. The nonlinear roll equation, which includes B1 type damping and quantic restoring, besides the wave excitation moment and moment generated by fins, was linearized for relative small roll angles. The role of PID controller was to generate the corrective roll moment through the controlled fins in order to stabilize the roll motion. The thresholds for the controller's gains were determined using the Laplace transform and Routh – Hurwitz criterion. A simple but precise iterative scheme was used for the rapid integration of the system equations of motion in three cases: only proportional (P) component, proportional and derivative (PD) components and full PID controller. The numerical simulations have showed that all the analysed variants achieved roll reduction satisfactorily.

K***ey words:*** ship, controler, numerical analysis.

1. INTRODUCTION

Stabilization of excessive ship roll motions induced by waves, winds and currents is of great importance because these oscillations may cause damage to the cargoes and equipment on board, would make the crew and passengers feel uncomfortable and eventually may capsize the ship.

During the last decades, many attempts have been made to reduce the ship rolling in a seaway. Of the systems of roll stabilization devised, only bilge keel, the gyroscope, anti-rolling tanks and activated fins were widely used in practice. The anti – rolling systems may be divided into two general categories, namely, passive and active. In the passive systems, no control devices are needed to develop the stabilizing moments. In the active systems, sensing elements are used to anticipate motion and to control the forces developed by stabilizers, [1 - 3].

Nowadays, stabilizing fins are the most effective and popular anti – rolling devices in use. The fins were initially applied on ocean liners where passenger comfort was a priority and on military vessels where stable gun platforms were needed but, as time went on, more and more ships were equipped with such stabilization system. The lift forces generated on fins will result in a stabilizing roll moment that counteracts the wave and wind perturbing moments in order to stabilize the ship. Since the lift force depends on the relative inflow speed, the stabilizing fins are effective only for relatively large ship forward speeds.

There are many control strategies for fin stabilizers. Representative conventional control schemes are the PID approach and its modified versions, [4, 5]. Advanced schemes include H_∞ control [6], neural networks [7], fuzzy control [8], adaptive sliding mode control [9] or particle swarm optimized PDD2 control, [10].

In the paper, using a linearized version of the roll equation, Laplace transform, Routh - Hurwitz criterion and a precise iterative scheme, we demonstrated that there is a wide range in the three-dimensional space of the PID controller gains for which the roll oscillations can be attenuated to acceptable values for all activities on board of the ship.

2. THE NONLINEAR ROLL EQUATION FOR A SHIP EQUIPPED WITH FIN STABILIZERS

The nonlinear roll equations suggested in the literature differ mainly in the way in which the damping and restoring moments are represented. In the present study, B1 type damping and quantic restoring are used so the roll equation can be expressed as

$$(I_{xx} + \delta I_{xx})\ddot{\theta} + B_L\dot{\theta} + B_N\dot{\theta}\left|\dot{\theta}\right| + \Delta(C_1\theta + C_3\theta^3 + C_5\theta^5) = M_w + M_f \quad (1)$$

with I_x and δI_x denoting the ship and added mass inertia in roll, θ the roll angle, B_L and B_N the linear and nonlinear damping coefficients, Δ the ship weight displacement, C_1, C_3 and C_5 the coefficients of the restoring moment, M_w the wave excitation moment and M_f the moment generated by the fin stabilizers.
In modelling the sea wave disturbance, we consider regular sinusoidal waves with no phase lag, so M_w is given by relation (2).

$$M_w = \omega_e^2 a_m I_{xx} \cos(\omega_e t) \tag{2}$$

where ω_e is the encounter frequency and a_m the maximum wave steepness. The fins stabilizer moment is given by relation (3).

$$M_f = \rho V_f^2 A_f R_f C_L(\alpha_e) \tag{3}$$

where ρ is the sea water density, A_f the fin area, R_f the fin moment arm, V_f the relative speed between the ins and the flow (it can be approximated with the ship forward speed, V) and $C_L(\alpha_e)$ the lift coefficient of the fin. The dependence of the coefficient C_L on the effective angle of attack α_e is approximately linear on the interval $\alpha_e \in [0, \alpha_{stall}]$, with α_{stall} being the stall angle (the angle from which the fin lift force begins to decrease). So we consider the relation (4).

$$C_L(\alpha_e) \cong \tilde{C}_L \cdot \alpha_e, \text{with} \tilde{C}_L = \partial C_L / \partial \alpha_e |_{\alpha_e = 0} \tag{4}$$

Finally, the angle α_e is defined as follows

$$\alpha_e = -\alpha_m - \alpha_{fa} \tag{5}$$

with α_m being the mechanical angle of the fins and α_{fa} the flow angle induced by the combination between the forward speed and roll rate. The last is given by relation (6).

$$\alpha_{fa} = arctan(R_f \dot{\varphi}/V) \cong R_f \dot{\varphi}/V \tag{6}$$

The actuation of the fin stabilizers is provided by a electro – hydraulic system, so the control of the fins is constrained by the characteristics of this system. The main constraints appear as the magnitude saturation α_{sat} (the maximum possible value of α_m), the slew rate saturation $\dot{\alpha}_{sat}$ (the maximum rate of α_m) and the time delay (the delay between the commanded control input, α_c, and the actual mechanical angle of the fin). These constraints can be incorporated in the first – order differential equation from relation (7).

$$T_e \dot{\alpha}_m + \alpha_m = K_{dc} \alpha_c \tag{7}$$

where T_e is the time constant of the actuator and K_{dc} the gain of the control input, and in the inequalities from relation (8).

$$|\alpha_m| \leq \alpha_{sat}, |\dot{\alpha}_m| \leq \dot{\alpha}_{sat}, |\alpha_e| \leq \alpha_{stall} \tag{8}$$

In conclusion, after dividing with $I_{xx} + \delta I_{xx}$, the nonlinear roll equation for the ship equipped with a pair of fin stabilizers is written as follows:

$$\ddot{\theta} + (b_L + K_\alpha R_f / V)\dot{\theta} + b_N \dot{\theta}|\dot{\theta}| + c_1\theta + c_3\theta^3 + c_5\theta^5 = m_0 \cos(\omega_e t) - K_\alpha \alpha_m \tag{9}$$

where

$$b_L = \frac{B_L}{I_{xx} + \delta I_{xx}}, b_N = \frac{B_N}{I_{xx} + \delta I_{xx}}, c_1 = \frac{\Delta\, C_1}{I_{xx} + \delta I_{xx}}, c_3 = \frac{\Delta\, C_3}{I_{xx} + \delta I_{xx}}, c_5 = \frac{\Delta\, C_5}{I_{xx} + \delta I_{xx}},$$

$$m_0 = \frac{\omega_e^2 a_m I_{xx}}{I_{xx} + \delta I_{xx}}, K_\alpha = \frac{\rho V^2 A_f R_f \tilde{C}_L}{I_{xx} + \delta I_{xx}}$$

with α_m provided from (7).

3. THE LINEARIZED ROLL EQUATION

For relative small roll angles θ, the nonlinear part of equation (9) can be neglected. In such a situation, the linearized version

$$\ddot{\theta} + (b_L + K_\alpha R_f / V)\dot{\theta} + \omega_n^2 \theta = m_0 \cos(\omega_e t) - K_\alpha \alpha_m \tag{10}$$

can be used. Here, $\omega_n = \sqrt{c_1}$ represents the ship natural frequency in roll.
Using the variables $x_1 = \theta, x_2 = \dot{\theta}$ and $x_3 = \alpha_m$, the equations (10) and (7) turn into the first – order system of differential equations

$$\begin{cases} \dot{x}_1 = x_2 \\ \dot{x}_2 = -\omega_n^2 x_1 - (b_L + K_\alpha R_f / V)x_2 + m_0 \cos(\omega_e t) - K_\alpha x_3 \\ \dot{x}_3 = k_2 x_3 + k_1 \alpha_c \end{cases} \quad 11)$$

with $k_1 = K_{dc}/T_e$ and $k_2 = -1/T_e$.

4. PID CONTROLLER

A proportional – integral – derivative (PID) controller is a control loop mechanism employing feedback that is widely used in industrial control systems to enhance their performance. A PID controller continuously calculates an error value $e(t)$ as the difference between a desired set point and a measured process variable and applies a correction.
In connection with the theme of our paper, figure 1 presents a block diagram of a PID controller applied to

the fin anti – rolling system (the plant). Here, $r(t)$ is the reference rolling input ($\varphi \cong 0$), $y(t)$ is the measured process value (the real angle $\varphi(t)$) and $e(t) = r(t) - y(t)$ is the error. Control $u(t)$ using a PID controller in continuous time takes the form of

$$u(t) = K_p e(t) + K_i \int_0^t e(\tau)d\tau + K_d \frac{d}{dt} e(t) \qquad (12)$$

where K_p, K_i and K_d are the proportional, integral and derivative gains, respectively. To tune these gains one can use either a manual adjustment or one of the following techniques: trial and error, the Niegler – Nichols method or the Cohen – Coon method. The different parts of the PID controller have different contributions. Thus, the proportional (P) controller can increase the response speed and improve the steady – state error slightly. The integral (I) controller can diminish the static error while the derivative (D) controller changes in a beneficial way the transient response.

Concerning our topic, the control over the ship stability against rolling may be exercised by means of the angle $\alpha_c = u(t)$.

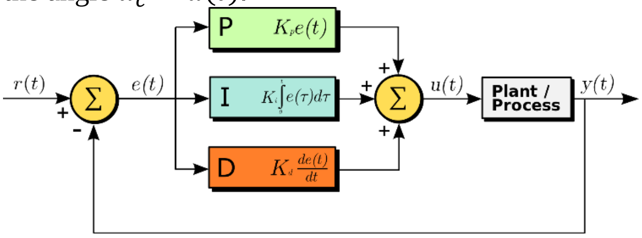

Fig. 1. A block diagram of a PID controller

5. ITERATIVE SCHEME OF NUMERICAL INTEGRATION

To solve the system (11) we used a simple iterative scheme based on backward differences for derivatives:

$$\begin{cases} x_1^{(n+1)} = x_1^{(n)} + x_2^{(n)} \cdot dt \\ x_2^{(n+1)} = x_2^{(n)}(1 - b_{Lm}dt) - \omega_n^2 x_1^{(n)} \cdot dt + m_0 cos(\omega_e t^{(n)})dt - K_\alpha x_3^{(n)} \cdot dt \\ x_3^{(n+1)} = x_3^{(n)}(1 + k_2 dt) + k_1 u^{(n)} \cdot dt \end{cases} \qquad (13)$$

where

$$b_{Lm} = b_L + K_\alpha R_f / V$$

$$u^{(n)} = K_p x_1^{(n)} + K_i dt \sum_{j=1}^{n} x_1^{(j)} + K_d \frac{x_1^{(n)} - x_1^{(n-1)}}{dt}$$

and dt is the time step of integration, [11].

6. THRESHOLDS FOR PID CONTROLLER GAINS BY LAPLACE TRANSFORM

One question that needs to be answered at this stage is: How to choose the gains K_p, K_i and K_d?

To give a solution, we applied the Laplace transform to the system consisting of equations (10) and (7), with $\alpha_c = u$ given by (12), and we obtain

$$\begin{cases} \Theta(s)(s^2 + b_{Lm}s + \omega_n^2) = \frac{m_0 s}{s^2 + \omega_e^2} - K_\alpha \Lambda(s) \\ \Lambda(s)(s - k_2) = k_1 \left(K_p + \frac{K_i}{s} + K_d s\right) \Theta(s) \end{cases}$$

with $\Theta(s) = \mathcal{L}(\theta(t))$ and $\Lambda(s) = \mathcal{L}(u(t))$. By eliminating $\Lambda(s)$, we get

$$\Theta(s) = \frac{m_0 s^2 (s - k_2)}{(s^2 + \omega_e^2)\left[s^4 + (b_{Lm} - k_2)s^3 + (\omega_n^2 - b_{Lm}k_2 + K_\alpha k_1 K_d)s^2 + \left(K_\alpha k_1 K_p - \omega_n^2 k_2\right)s + K_\alpha k_1 K_i\right]}$$

In order to have a bounded solution, it is necessary that the roots of the denominator of the function $\Theta(s)$ have negative real parts or at most zero. The Routh – Hurwitz criterion provides the necessary and sufficient conditions for this to occur. Thus, for a cubic polynomial $p(s) = s^3 + \alpha_2 s^2 + \alpha_1 s + \alpha_0$, the required conditions are $\alpha_0 > 0$, $\alpha_2 > 0$ and $\alpha_1 \alpha_2 > \alpha_0$. For a fourth polynomial $p(s) = s^4 + \alpha_3 s^3 + \alpha_2 s^2 + \alpha_1 s + \alpha_0$, the same conditions are as follows: $\alpha_0 > 0$, $\alpha_3 > 0$, $\alpha_2 \alpha_3 > \alpha_1$ and $\alpha_1 \alpha_2 \alpha_3 > \alpha_0 \alpha_3^2 + \alpha_1^2$.

<u>Case 1</u>: $K_p \neq 0, K_i = K_d = 0$

One has bounded solutions only if

$$\alpha_0 = K_\alpha k_1 K_p - \omega_n^2 k_2 > 0$$

$$\alpha_2 = b_{Lm} - k_2 > 0$$

$$\alpha_1 \alpha_2 - \alpha_0 = b_{Lm}\omega_n^2 - b_{Lm}^2 k_2 + b_{Lm} k_2^2 - K_\alpha k_1 K_p > 0$$

The first two conditions are satisfied for any K_p ($k_2 < 0$), while the last requires that

$$K_p < b_{Lm}(\omega_n^2 + k_2^2 - b_{Lm}k_2)/K_\alpha k_1 \quad (14)$$

Case 2: $K_p \neq 0, K_d \neq 0, K_i = 0$

The boundless of the solutions requires that the pair (K_p, K_d) verify the inequality:

$$K_\alpha k_1 K_p + K_\alpha k_1(k_2 - b_{Lm})K_d + b_{Lm}(b_{Lm}k_2 - k_2^2 - \omega_n^2) < 0 \quad (15)$$

Case 3: $K_p, K_d, K_i \neq 0$

According to Routh – Hurwitz criterion, bounded solutions requires that the triplet (K_p, K_d, K_i) checks the condition (15) together with

$$(K_\alpha k_1 K_p - \omega_n^2 k_2)(\omega_n^2 - b_{Lm}k_2 + K_\alpha k_1 K_d)(b_{Lm} - k_2) > K_\alpha k_1 K_i (b_{Lm} - k_2)^2 + (K_\alpha k_1 K_p - \omega_n^2 k_2)^2 \quad (16)$$

7. NUMERICAL SIMULATIONS

To check the effectiveness of the fin stabilizer system in reducing the roll amplitudes, we performed a number of numerical simulations for a fishing vessel [4]. Non-dimensional damping and restoring moment coefficients are as

$$b_L = 0.069, b_N = 0.01, c_1 = 1.204, c_3 = -1.8, c_5 = 0.61$$

while the data for the fin system are

$$k_1 = 2.7322, k_2 = -k_1, \rho = 1025\ kg/m^3, A_f = 2.5\ m^2, R_f = 3.7\ m, \tilde{C}_L = 1.9$$

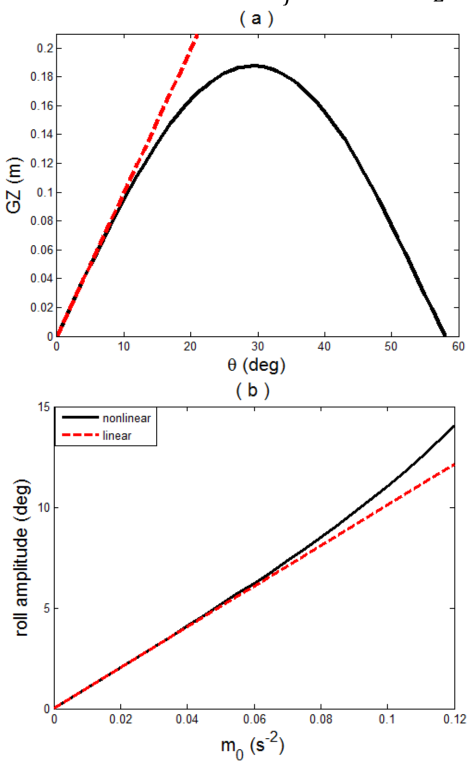

Fig. 2. (*a*) The righting arm curve of the fishing boat; (*b*) Roll amplitude versus wave amplitude.

The red dashed lines are associated to the linear model.

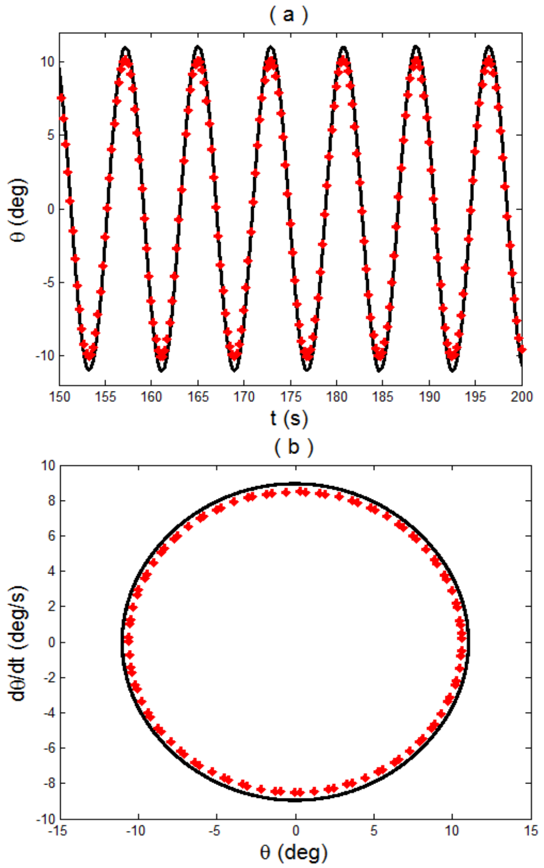

Fig. 3. (*a*) The time evolution of roll angle for $m_0 = 0.1$; (*b*) The phase plane $(\theta, \dot{\theta})$.

The red stars are associated to the linear model.

For the sinusoidal wave parameters, we selected the values $m_0 = 0.1$ and $\omega_e = 0.8$ but similar results can be obtained in all situations where the linear approximation is acceptable.

Figure 2*a* presents the righting arm curve associated to the quantic restoring moment. Its linear approximation (dashed red line) stays close to the curve for roll angles not exceeding 15^0. In the absence of fin stabilizer and for fixed encounter frequency $\omega_e = 0.8$, the roll amplitude increases almost linearly with m_0, as suggested in figure 2*b*. The linearization effect of the equation of motion is felt starting with $m_0 = 0.08$. Thus, for $m_0 = 0.1$ the nonlinear roll equation yields the amplitude $a_\theta = 11.02^0$ while its linearized version gives $a_\theta = 10.3^0$ (see figures 3*a* and 3*b*).

The main part of this section refers to the influence of the gains K_p, K_d and K_i on the amplitude of the ship roll motion. Our study contains three cases, namely:

Case 1: $K_p \neq 0, K_i = K_d = 0$

Since b_{Lm} and K_α depend on the ship velocity V, the relation (14) provides the maximum value of the coefficient K_p for each velocity so that the roll amplitude remains finite. Figure 4*a* shows an inverse proportionality between speed V and gain K_p. When condition (14) ceases to be verified, the amplitude of roll oscillation increases very rapidly, no matter it is calculated by the iterative scheme (13) or by integration of system (11) (with *ode 45* in Matlab). Figure 4*b* further shows that below this threshold for K_p, the roll amplitude decreases with increasing K_p. This trend is accentuated by high ship speeds (for which, additionally, the damping b_{Lm} is significantly increased). Regarding the mechanical angle of fins, α_m, and the effective angle of attack, α_e , every time the condition (14) is checked and the speed of the ship exceeds 2 m / s, they remain at low values, which satisfy the constraints (8), as shown in figures 4*c* and 4*d*.

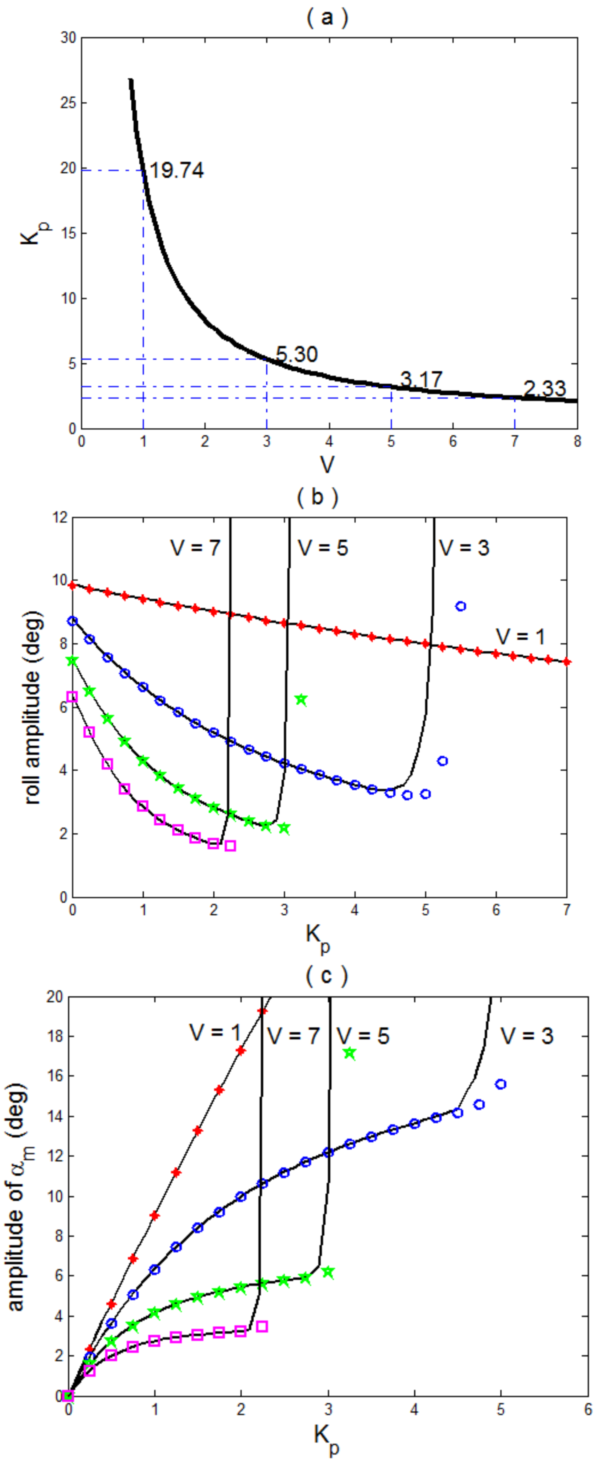

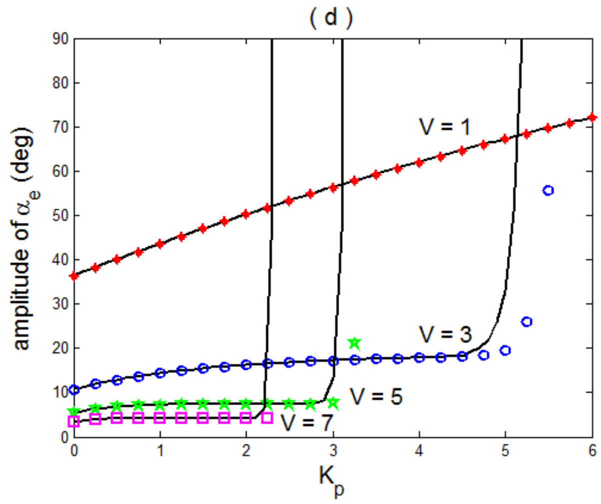

Fig. 4. (*a*) The threshold for gain K_p; The roll amplitude (*b*), the amplitude of mechanical angle of fin (*c*) and of the effective angle of fin (*d*) as a function of gain K_p, for different ship speed *V*

What actually happens in the vicinity of the threshold indicated by (14)? We will clarify this aspect for, say, *V* = 5, when the critical threshold is $\left(K_p\right)_{crit} = 3.17$ (see figure 4*a*). If K_p is significantly smaller than $\left(K_p\right)_{crit}$, then the solutions provided by (11) and (13) indicate a harmonic oscillation of frequency ω_e. Except for the roots $\pm i\omega_e$, the other roots of the denominator of fraction $\Theta(s)$ have strictly negative real parts (see figure 5*d*). Figure 5*a* , obtained for $K_p = 2$, captures the excellent agreement between the two solutions.
In the vicinity of the critical value, two more roots have real parts close to zero, so the solution will be an overlap of two harmonics of different frequencies and amplitudes. The systems (11) and (13) give bounded but different solutions, as presented in figure 5*b* for $K_p = 3$.
Once the threshold $\left(K_p\right)_{crit}$ is exceeded, the solution of (11) contains a component of form $e^{at}cos(\omega t + \varphi), a > 0$, which makes it boundless (see figure 5*d* for $K_p = 3.2$).

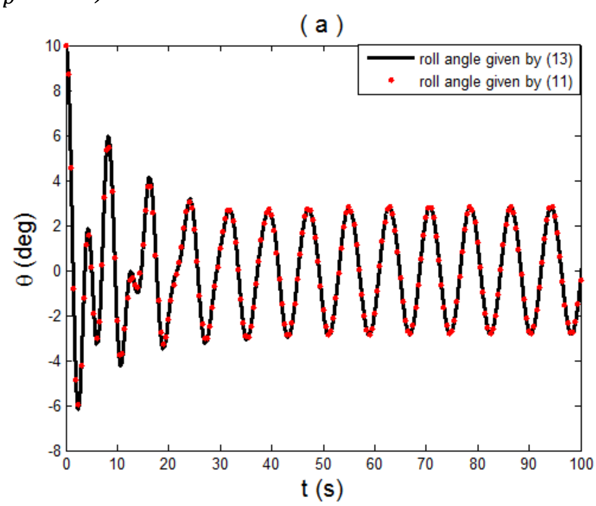

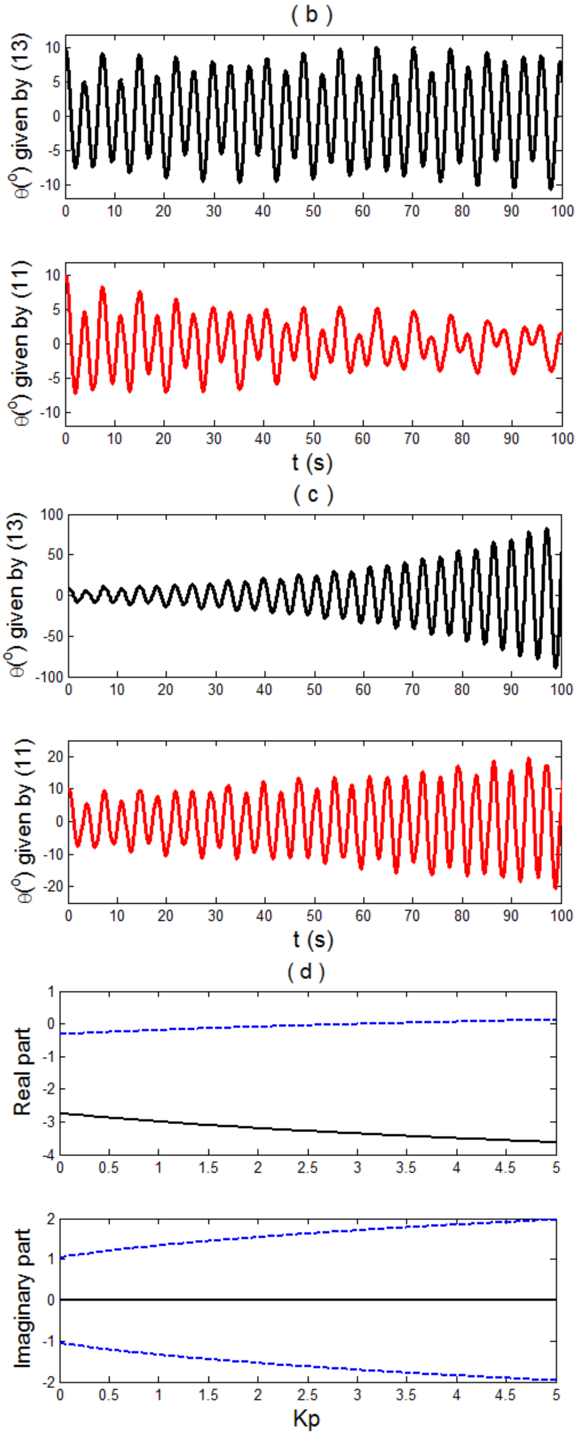

Fig. 5. The time evolution of roll angle for $(a)\ K_p = 2$; $(b) K_p = 3$; $(c) K_p = 3.2$. (d) The real and imaginary parts of denominator of fraction $\Theta(s)$ as a function of gain K_p

<u>Case 2</u>: $K_p \neq 0, K_d \neq 0, K_i = 0$

For each ship speed V, relation (15) defines in the plane (K_p, K_d) an infinite trapezoidal surface situated between the axes $K_p = 0, K_d = 0$ and the inclined line associated with the inequality. Figure 6*a* shows the relative position of these surfaces for $V \in \{1,3,5,7\}$. Using only D controller causes the roll amplitude to decrease with K_d, regardless the speed V. There are no limitations for K_d and the roll amplitude decrease is more pronounced for higher speeds V, as indicated in figure 6*b*.

Figure 7 presents the roll amplitude and the mechanical angle of fin for different pairs (K_p, K_d) and $V = 5$. The right triangle in the right-down part of each panel corresponds to the pairs (K_p, K_d) for which the denominator of fraction $\Theta(s)$ has two complex conjugate roots with positive real part (unbounded solution; consider these panels in connection with figure 6*a*). It should be noted that for the vast majority of pairs (K_p, K_d) in the above-mentioned trapezoidal area, the PD controller ensures a substantial reduction in the initial roll amplitude of 10.3^0.

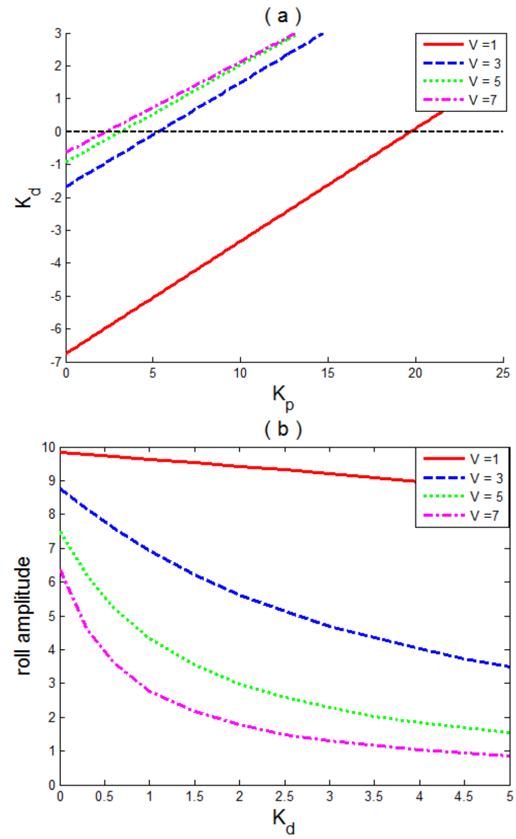

Fig. 6. (a) The threshold for gains (K_p, K_d) for different ship speeds; (b) The roll amplitude as a function of gain K_d, if only D controller is activated

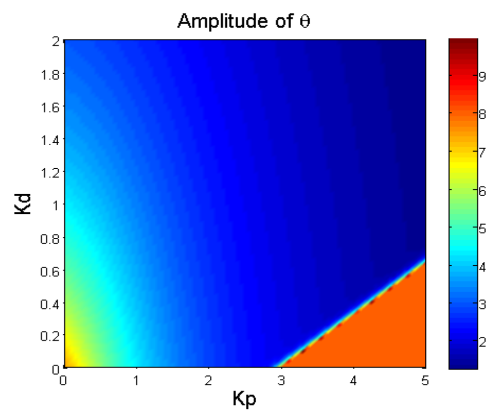

a)

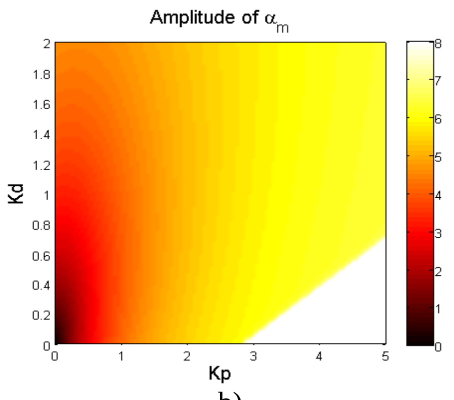

b)

Fig. 7. The roll amplitude (a) and the amplitude of mechanical angle of fin (b) as a function of gains K_p and K_d, for the ship speed $V = 5$

<u>Case 3</u>: $K_p, K_d, K_i \neq 0$

This time, the denominator of fraction $\Theta(s)$ is a sixth degree polynomial so it can have, in addition to the complex roots, $\pm i\omega_e$, two or four complex roots. The boundary of condition (16) represents, for each gain K_i, a parabola in the plane (K_p, K_d). As K_i increases, the area corresponding to finite roll amplitudes decreases, as shown in figures 8 and 9, obtained for $K_i = 1$ and $K_i = 2$, respectively. Below the boundary defined by (16), the number of roots with positive real part is always two (pink area in figures 8b and 9b).

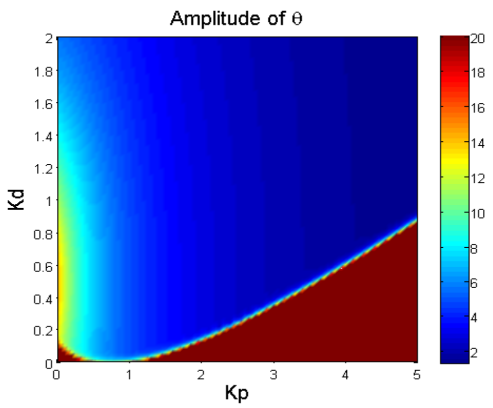

a)

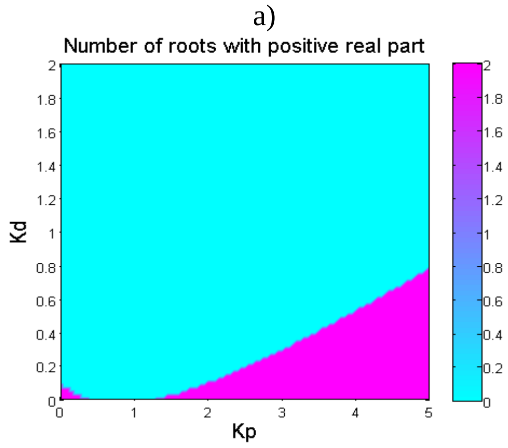

b)

Fig. 8. The roll amplitude (a) and the number of roots of the denominator of fraction $\Theta(s)$ with positive real parts (b) for $V = 5$ and $K_i = 1$

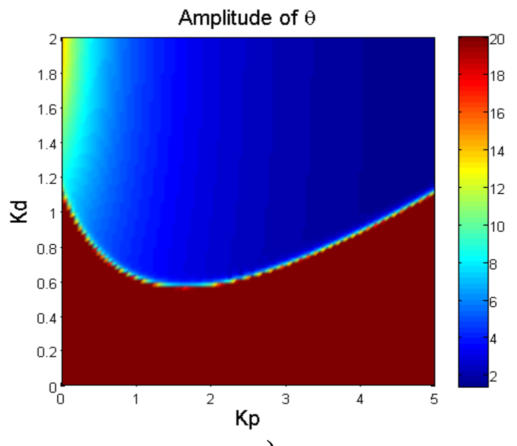

a)

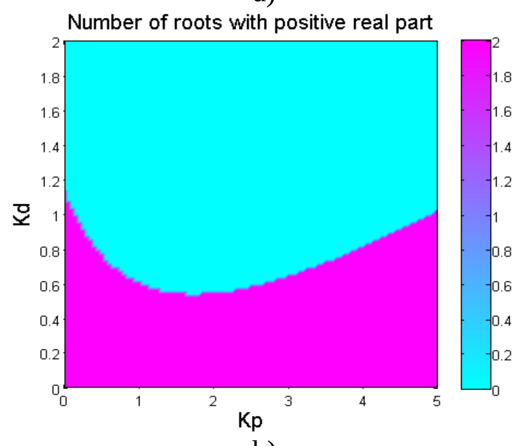

b)

Fig. 9. The same as in figure 8, but for $K_i = 2$

Note, in addition, the existence of a narrow area, for small K_p, in which the roll oscillations do not attenuate (on contrary, sometimes they intensify).

For the most part of the domain (K_p, K_d, K_i) in which the solution of (11) is bounded, the roll amplitudes have been reduced to acceptable values of 1^0 to 4^0. Changing the parameters of the PID controller influences, to some extend, the transition to the steady stare and the roll amplitude, as shown in figure 10.

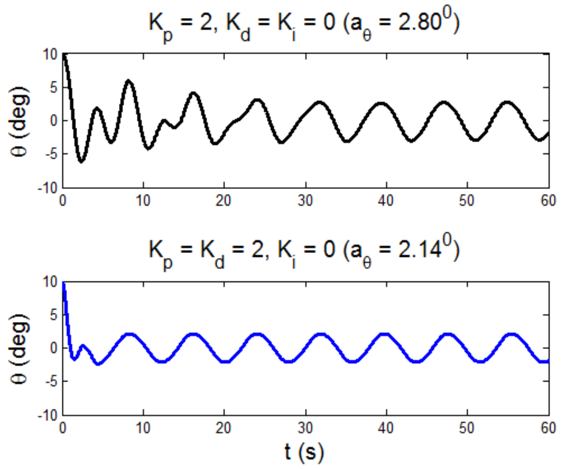

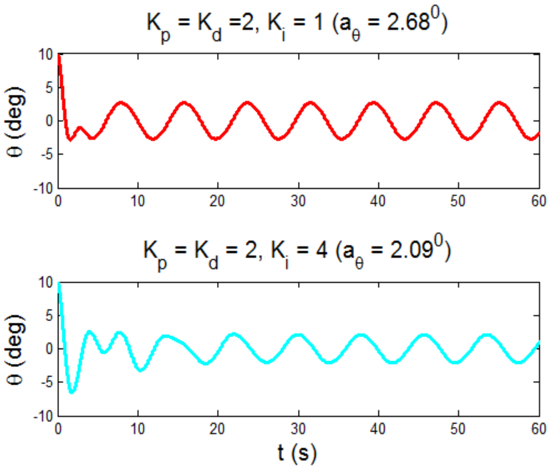

Fig. 10. The time evolution of roll angle for different gains (K_p, K_d, K_i) and $V = 5$

8. CONCLUSIONS

In the paper, a one – dimensional nonlinear model was derived to study the roll motion of a ship equipped with fin stabilizers. For roll angles less than 10^0 – 15^0, the model can be linearized without introducing significant errors. A PID control algorithm was applied to reduce the roll motion of a fishing ship sailing in regular waves. Using the Laplace transform, we deduced in the three dimensional space of the PID controller parameters a paraboloid – like surface that separates the domain leading to a significant reduction of the roll amplitudes from that associated with boundless solutions. This surface is determined only by the ship parameters (including the fins), the properties of the fin's actuator and the forward speed of the ship. The frequency and amplitude of the sea wave are involved only in the shape of the ship's response, both in transition and in steady – state phases.

In addition, numerical simulations, based on a simple, fast and accurate iterative scheme, showed that:

a) the stabilizing fins are effective only for relatively high speeds of the ship;

b) as the ship speed increases, the volume occupied by the triplets (K_p, K_d, K_i) near the origin for which the roll amplitudes are finite is reduced;

c) simple controllers, having only component P and possibly D, seem to be sufficient for a significant attenuation of the roll oscillations. At least in the case under analysis, component I has a rather negative effect.

9. REFERENCES

1. Kula K S (2015). *An overview of roll stabilizers and systems for their control*, TransNav, The Int. J. on Marine Navigation and Safety of Sea Transportation, 9(3), 405 – 414.

2. Perez T (2005). *Ship motion control* Springer – Verlag, London.

3. Marzouk O A and Nayfeh A H (2014). *Control of ship roll using passive and active anti – roll tanks*, Ocean Engineering, 36(9), 661 – 671.

4. Ghassemi H, Malekizade H and Ashrafi A (2016). *Control of roll motion of fishing vessel by fin – stabilizer using PID controller*, Int. J. of Physics, 4(6), 181 – 186.

5. Alarcin F, Demirel H, Ertugrul M and Yurtseven A (2014). *Conventional PID and modified PID controller design for roll fin electro – hydraulic actuator*, Acta Polytechnica Hungarica, 11(3), 233 – 248.

6. Hickey N A, Grimble M J, Johnson M A, Katebi M R and Melville R (1997). *Robust fin roll stabilization of surface ships*, Proceedings of the 36th Conference on the Decision and Control San Diego, SUA, pp 4225 – 4230.

7. Alarcin F (2007). *Internal model control using neural network for ship roll stabilisation*, J. Mar. Sci. Tech., 15, 141 – 147.

8. Sutton R, Robert G N and Dearden SR (1989). *Design study of a fuzzy controller for ship roll stabilization*, Electronic and Communication Engineer Journal, 12, 159 – 166.

9. Moradi M and Malekizade H (2013). *Robust adaptive first – second order sliding mode control to stabilize the uncertain fin – roll dynamic*, Ocean Engineering, 69, 18 - 23.

10. Ertogan M, Ertugrul S and Taylan (2016). *Application of particle swarm optimized PDD2 control for ship roll motion with active fins*, IEEE/ASME Trans. Mechatron, 21, 1004 – 1-14.

11. Deleanu D, Panaitescu M and Panaitescu F V (2020). *An accurate and fast iterative scheme for estimating the ship rolling and capsizing in regular waves* IOP Conference Series: Material Science and Engineering, 916(1), article number 012025.

Received: April 28, 2022 / Accepted: December 15, 2022 / Paper available online: December 20, 2022 © International Journal of Modern Manufacturing Technologies